ISSN: 2414-1895 DOI: 10.6919/ICJE.202411_10(11).0005

Research on the Mechanism Motion and Structural Stiffness of Shield Segment Erector

Shutao Yu, Liying Deng, and Xin Wang

College of Chemical Equipment, Shenyang University of Technology, Shenyang, Liaoning 111027, China

Abstract

To validate whether the load characteristics of the shield segment erector meet the design specifications, this study conducted a detailed analysis of torque requirements under four typical working conditions. First, focusing on the functional requirements and operational behavior of the erector, a detailed 3D model was created using 3D design software. Next, the erector's structure was simplified, with its load-bearing conditions approximated by a simply supported beam model, leading to the derivation of corresponding torque calculation formulas and the computation of the required design torque values. Finally, static structural analysis of the erector's stiffness under four load scenarios was carried out using ANSYS software. The results revealed that under the maximum load condition, the erector experienced a maximum stress of 213.74 MPa and a maximum displacement of 1.6 mm, both of which are within the safe range and meet the structural strength requirements.

Keywords

Segment Erector; Loading Conditions; Simply Supported Beam Model; Stiffness Analysis.

1. Introduction

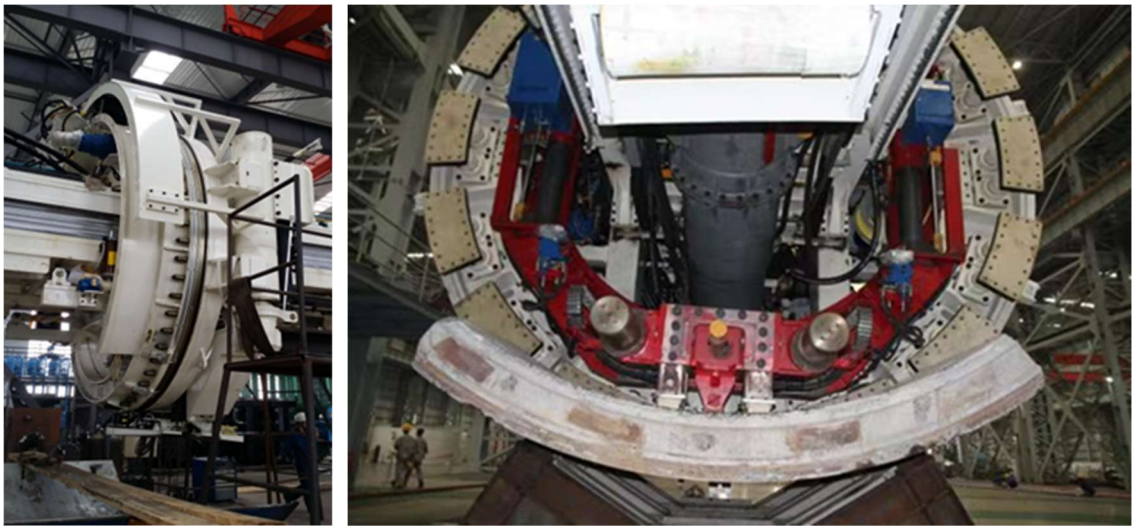

Figure 1. Circular Shield Segment Erector

As the process of urbanization rapidly advances, large metropolitan areas, urban clusters, and regional hub cities are increasingly interconnected, leading to a significant rise in global demand for large-scale shield tunneling construction [1]. As one of the methods for utilizing underground space, the shield tunneling method involves the advancement of a shield machine through the ground. The

ISSN: 2414-1895 DOI: 10.6919/ICJE.202411_10(11).0005

surrounding rock is supported by the shield shell and segments to prevent tunnel collapse. The shield machine is an indispensable tool for its efficient operation [2]. This method significantly accelerates construction speed. As a critical component of the shield machine, the development and manufacturing of the segment erector are essential tasks. Due to the even distribution of forces, accurate assembly, and convenient operation of segments in circular cross-section tunnels, this design is favored by shield machine manufacturers both domestically and internationally. As a result, almost all shield machine construction cross-sections are circular, and this approach has developed rapidly, reaching a very mature stage [3], as shown in Figure 1.

In the study of the mechanism motion of the segment erector, Song. C.B. addressed the shortcomings of traditional translation mechanisms with large spans and poor load performance [4], proposed an optimized design featuring dual arms with dual cylinders and a simply supported beam-type guide rod. This significantly reduced the overall span of the translation mechanism in the entire machine. Liu. F.X. from China Railway Construction Heavy Industry addressed the issues of low efficiency in manual segment grabbing and the difficulty in ensuring assembly quality by proposing an intelligent grabbing and assembly algorithm for the segment erector based on the contouring method [5]. By measuring system parameters, he derived the motion state equations for the erector and the corresponding stroke equations for the fine-tuning system cylinders, thereby achieving automation and precision in the segment grabbing and assembly posture adjustment. Xia. Y.M. and colleagues from Central South University studied the dynamic simulation process of the entire machine and analyzed the stiffness performance of the suction cups and clamping frames of the segment erector in different assembly postures [6]. Wang. D.Z. and colleagues first established a model for the fine-tuning mechanism of the erector [7]. They used kinematic analysis software to perform dynamic simulations of the model under load conditions, determining the thrust values of the two drive cylinders in the fine-tuning mechanism and validating the accuracy of the developed model. Yuan et al. established a 3-SPS-1 model for the fine-tuning mechanism of the segment erector [8]. By creating parameterized pose parameters for both stiffness and rotational motion, they obtained the loading conditions of each component during the assembly process and used these as boundary conditions for the dynamic system strength verification. Li Gang et al. conducted simulation studies on the kinematics and dynamics of the segment erector [9]. They derived the velocity and driving force curves for each active component and analyzed their mechanical properties. Liao S.M. et al. conducted field measurements of the entire process of shield segment assembly and the structural stress characteristics after assembly by setting up a full-section tunnel test ring in a deep-buried segment of typical strata [10]. They analyzed the variation patterns of internal forces during the segment assembly process. Due to the fact that the segment erector is in different positions and configurations while performing various actions during its overall rotational movement, the torque experienced by the erector varies accordingly, therefore, this paper analyzes and calculates the required torque of the segment erector under various operating conditions, considering the erector's different actions to complete its corresponding functions. Additionally, it performs a static structural strength analysis of the clamping frame during the segment grabbing process.

2. Overview and Condition Analysis of the Segment Erector

2.1 Assembly Principle of the Segment Erector

The paper primarily investigates the design and functionality of a vacuum suction cup-type circular segment erector with a diameter of 7.6 meters. This erector is required to perform six fundamental movements, horizontal translation, axial rotation, vertical lifting, fore-and-aft tilting, lateral inclination, and lateral deflection, corresponding to the six degrees of freedom needed for segment handling. The designed structure must support segment grabbing, positioning, and fine-tuning, as illustrated in Figure 2.

ISSN: 2414-1895 DOI: 10.6919/ICJE.202411_10(11).0005

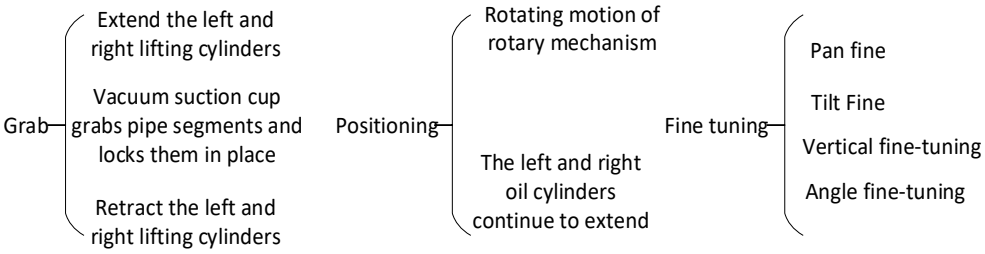

Figure 2. Functional Classification of the Segment Erector

The workflow for segment assembly is as follows: The segment erector translates to the segment position→ The left and right lifting cylinders extend→ Grab the segment and secure it→ Retract the lifting cylinders→ Move to the assembly area→ Rotate the erector→ Extend the lifting cylinders→ Continue the rotation mechanism's movement→ Perform fine-tuning with the adjustment mechanism→ Position the segment in place→ Retract the lifting cylinders→ Rotate the erector back to the initial position. At this point, the complete assembly of the segment ring is finished. Figure 3 below shows the completed ring assembly.

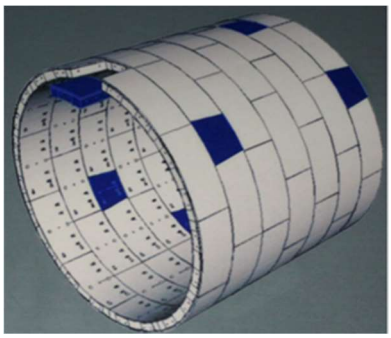

Figure 3. Complete Ring Assembly Diagram

2.2 Structural Design of the Segment Erector

Whether it is the diameter of the tunnel excavation, the overall structure of the segment erector, or its functional movements, the design remains consistent with traditional models. Installed at the tail of the shield, it is capable of assembling the segments into place, thereby completing the lining protection of the excavated tunnel [11]. Since the study focuses on circular cross-sections, the final design of the shield segment erector, considering tunnel dimensions, spatial constraints, degrees of freedom, and segment partitioning requirements, is illustrated in Figure 4. The main structural components include the support frame, translation mechanism, rotation mechanism, lifting mechanism, fine-tuning structure, and vacuum suction cups.

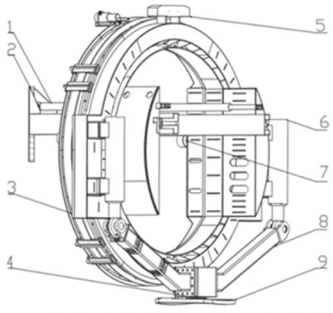

1. Translation mechanism; 2. bracket; 3. swing mechanism; 4. Trimming mechanism; 5. balancing weight; 6. Weightlifting mechanism; 7. Drive motor assembly; 8. choke; 9. Vacuum suction cup

Figure 4. Overall structure of the erector

ISSN: 2414-1895 DOI: 10.6919/ICJE.202411_10(11).0005

The segment erector uses the horizontal support in the translation mechanism to move forward and backward. This support utilizes a roller mechanism within the structure, with horizontal hydraulic cylinders as the driving force. The hydraulic cylinders connect the erector's main body to the support frame attached to the shield's tail. This setup enables movement along the horizontal main beam track on the support frame.

The horizontal main beam in the support frame provides all the support for the entire machine. The structure consists of symmetrically arranged channel beams on both sides and an I-beam that supports the overall machine structure. The main beam is fixed and connected to the internal part of the erector, and the inner sections of the two horizontal beams are equipped with channel-shaped structures to ensure the proper track for the roller movement.

The assembly machine utilizes the turntable mechanism's slewing support to achieve rotational operations. This part is fixedly connected to the internal gear ring of the slewing support and is powered by a hydraulic motor, which drives the carriage to perform circumferential rotational movement.

The lifting mechanism on both sides consists of two hydraulic cylinders each, used for extending to grab the segments and perform coarse adjustment and positioning for installation. The fine-tuning mechanism in the center of the frame is used to place the segments and make precise adjustments, connecting the segment to be installed with the assembled segments using custom bolts. According to the design requirements, the total weight of the segment assembly machine is 70 tons, and the weight of the segments being handled is 4 tons.

3. Analysis of Working Conditions of the Erector

In order to realize the completion of the above 6 basic assembly actions, the assembly machine has different working conditions when the translation mechanism, rotating mechanism, lifting mechanism and fine-tuning structure are in different positions and different loads. During the actual construction process. It is divided into the following working conditions: static load condition, dynamic load condition 1, dynamic load condition 2, dynamic load condition 3.

The first condition: static load (grasping segment) condition. This working condition is a kind of working condition analysis when the erector completes the function of grasping tube segments. In this working condition, the motion state of the segment assembler is: the left and right lifting cylinders in the lifting arm extend, rotate counterclockwise, the vacuum suction cup at the bottom grabs the segment, the side of the segment compacts the seal, and maintains a static state. Due to the static state under this working condition, certain pressure bearing and internal friction torque inside the rotating support will appear at the segment seal strip. As is shown in Figure 5. The mechanical equilibrium diagram is shown in Figure 6 below.

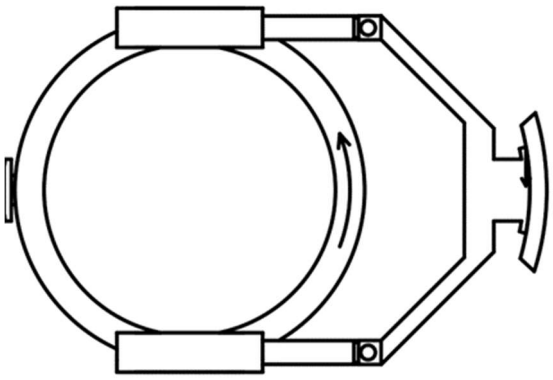

Figure 5. Working condition 1

ISSN: 2414-1895 DOI: 10.6919/ICJE.202411_10(11).0005

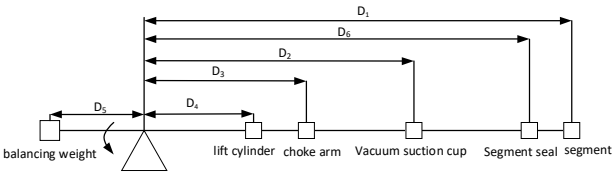

Figure 6. Schematic diagram of mechanical equilibrium under working condition

The final torque can be obtained from the mechanical equilibrium diagram:

$$M_T = (G_a \times D_1 + G_b \times D_2 + G_c \times D_3 + G_d \times D_4 - G_e \times D_5)/100 + F_1 \times D_6/1000 + M_f \quad (1)$$

The meaning contained in mathematical expressions:
G_a -Segment self gravity, KN ; D_1 -Distance from segment centroid to erector center of rotation, mm ; G_b -Vacuum suction cup gravity, KN ; D_2 -Distance from the center of gravity of the vacuum chuck to the center of rotation (hydraulic cylinder extension stroke), mm ; G_c -Choke arm gravity, KN ; D_3 -Distance from choke arm to center of rotation, mm ; G_d -Lift the hydraulic cylinder gravity, KN ; D_4 -Lift the hydraulic cylinder to the center of rotation, mm ; G_e -Top counterweight weight, KN ; D_5 -Distance from the weight of the top weight to the center of rotation, mm ; F_1 -The bearing capacity of the segment seal when the vacuum suction cup grabs heavy objects, KN ; D_6 -Distance from seal to center of rotation, mm ; M_f -Internal friction torque inside the rotary bearing, $KN \bullet m$.

Table 1 lists the design parameters.

Table 1. Parameter table of working condition 1

The weight of the segment itself G_a/T	4
The distance from the centroid of the segment to the center of rotation of the erector D_1/mm	4375
Weight of the vacuum sucker G_b/T	0.9
The distance between the center of gravity of the vacuum chuck and the center of rotation D_2/mm	3975
Choke arm weight G_c/T	6
The distance from the choke arm to the center of rotation D_3/mm	3500
Lift the hydraulic cylinder weight G_d/T	6.8
Lift the hydraulic cylinder to the center of rotation D_4/mm	400
Top counterweight weight G_e/T	4.7
The distance from the top counterweight weight to the center of rotation D_5/mm	2750
Segment seal bearing capacity F_1/KN	79.5
Distance from seal to center of rotation D_6/mm	4950
Seal strength δ $/KN/m$	53
Segment length L/m	1.5
Internal friction torque inside the rotary bearing $M_{fj}/KN \bullet m$	15

ISSN: 2414-1895 DOI: 10.6919/ICJE.202411_10(11).0005

(In the table, the pressure bearing of the segment seal strip is calculated as follows: Segment seal bearing capacity F_1 = Seal strength $\delta \times$ Segment length L ,The sealing strength refers to the stability and durability of the vacuum degree that the vacuum sucker can maintain during use.)

Bring the above parameters into (1), The erector torque M_T under the available working condition is $727KN \bullet m$.

The second working condition: dynamic load 1 working condition. To achieve the requirements of the positioning function of the erector, the rotary mechanism inside the erector rotates at a relatively small speed and can slowly move to the area where the segment is to be installed. Under this working condition, the motion state of the erector is: the left and right sides of the lifting hydraulic cylinder extend, while the rotating mechanism moves counterclockwise, and the vacuum sucker grabs the tube segment, thus driving the tube segment to move counterclockwise. Since it is a moving and rotating motion, the pressure generated by the segment seal is not taken into account during this process. However, the internal friction torque is also supported by the internal rotation of the erector. The working condition of dynamic load 1 is shown in the figure.

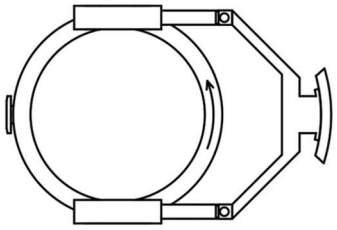

Figure 7. Working conditions 2

The schematic diagram of force analysis is shown in Figure 8 below:

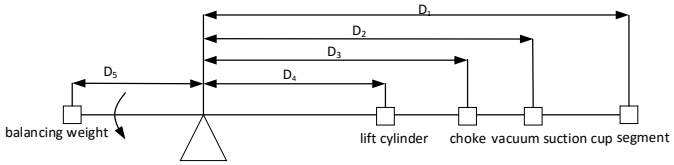

Figure 8. Schematic diagram of mechanical equilibrium in the second working condition 2

According to the above mechanical analysis diagram, the final torque of the erector under working condition 2 can be obtained.

$$M_1 = (G_a \times D_1 + G_b \times D_2 + G_c \times D_3 + G_d \times D_4 - G_e \times D_5) / 100 + M_1 \quad (2)$$

The meaning contained in mathematical expressions:

G_a -Segment self gravity, KN ; D_1 -Distance from segment centroid to erector center of rotation, mm ; G_b -Vacuum suction cup gravity, KN ; D_2 -Distance from the center of gravity of the vacuum chuck to the center of rotation (hydraulic cylinder extension stroke), mm ; G_c -Choke arm gravity, KN ; D_3 -Distance from choke arm to center of rotation, mm ; G_d -Lift the hydraulic cylinder gravity, KN ; D_4 -Lift the hydraulic cylinder to the center of rotation, mm ; G_e -Top counterweight weight, KN ; D_5 -Distance from the weight of the top weight to the center of rotation, mm ; M_1 -Internal friction torque inside the rotary bearing, $KN \bullet m$.

ISSN: 2414-1895 DOI: 10.6919/ICJE.202411_10(11).0005

Table 2 lists the design parameters.

Table 2. Parameter table of working condition 2

The weight of the segment itself G_a / T	4
The distance from the centroid of the segment to the center of rotation of the erector D_1 / mm	4375
Weight of the vacuum sucker G_b / T	0.9
The distance between the center of gravity of the vacuum chuck and the center of rotation D_2 / mm	3975
Choke arm weight G_c / T	6
The distance from the choke arm to the center of rotation D_3 / mm	3500
Lift the hydraulic cylinder weight G_d / T	6.8
Lift the hydraulic cylinder to the center of rotation D_4 / mm	400
Top counterweight weight G_e / T	4.7
The distance from the top counterweight weight to the center of rotation D_5 / mm	2750
Internal friction torque inside the rotary bearing $M_1 / KN \bullet m$	15

Using the above parameters in (2), the assembly machine torque under working condition two is obtained as 334 $KN \bullet m$.

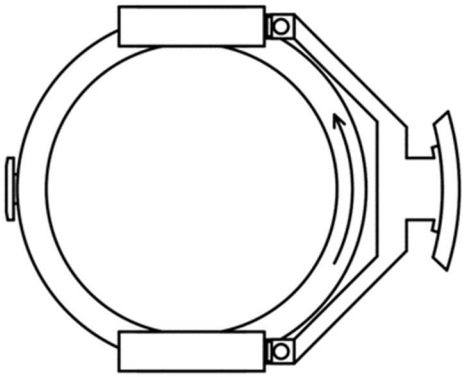

Figure 9. Working conditions 3

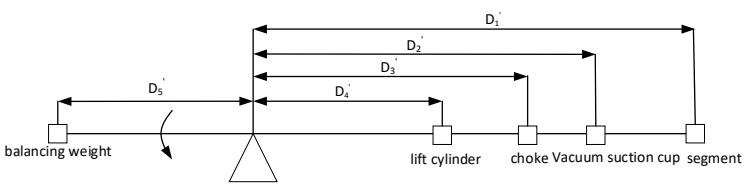

Figure 10. Mechanical Equilibrium Diagram for Condition 3

ISSN: 2414-1895 DOI: 10.6919/ICJE.202411_10(11).0005

Third condition: Dynamic Load Condition 2. After the vacuum suction cup grasps the segment, the assembly machine's rotary mechanism rotates at a higher speed, enabling the segment to be quickly moved to the installation position. Under this working condition, the movement of the assembly machine is as follows: the lifting cylinders on both sides retract, while the slewing support rotates counterclockwise, driving the segment grasped at the bottom to rotate. In this working condition, as the assembly machine is in motion, it is also subjected to the internal frictional torque M_1 within the rotary support of the assembly machine. As shown in Figure 9 below, it is a motion diagram under this working condition. The mechanical diagram is shown in Figure 10 below.

From the above mechanical equilibrium diagram, the final torque of the assembly machine can be determined.

$$M_2 = (G_a \times D_1^{'} + G_b \times D_2^{'} + G_c \times D_3^{'} + G_d \times D_4^{'} - G_e \times D_5^{'}) / 100 + M_1 \quad (3)$$

The meaning contained in mathematical expressions:

G_a -Segment self gravity, KN ; $D_1^{'}$ -The distance from the centroid of the segment to the rotary center of the assembly machine (hydraulic cylinder retraction stroke), mm ; G_b -The weight of the vacuum suction cup, KN ; $D_2^{'}$ -The distance from the center of gravity of the vacuum suction cup to the rotary center (hydraulic cylinder retraction stroke), mm ; G_c -The weight of the choke arm, KN ; $D_3^{'}$ -The distance from the support arm to the rotary center (hydraulic cylinder retraction stroke), mm ; G_d -The weight of the lifting hydraulic cylinder, KN ; $D_4^{'}$ -The distance from the lifting hydraulic cylinder to the rotary center (hydraulic cylinder retraction stroke), mm ; G_e -Top counterweight weight, KN ; $D_5^{'}$ -The distance from the top counterweight block to the rotary center (hydraulic cylinder retraction stroke), mm ; M_1 -Internal frictional torque of the slewing bearing, $KN \bullet m$.

The following are the design parameters, as shown in Table 3 below.

Table 3. Working Condition 3 Parameters

The weight of the segment itself G_a / T	4
The distance from the centroid of the segment to the center of rotation of the erector $D_1^{'} / mm$	2960
Weight of the vacuum sucker G_b / T	0.9
The distance between the center of gravity of the vacuum chuck and the center of rotation $D_2^{'} / mm$	2125
Choke arm weight G_c / T	6
The distance from the choke arm to the center of rotation $D_3^{'} / mm$	1815
Lift the hydraulic cylinder weight G_d / T	6.8
Lift the hydraulic cylinder to the center of rotation $D_4^{'} / mm$	-213
Top counterweight weight G_e / T	4.7
The distance from the top weight weight to the center of rotation $D_5^{'} / mm$	2750
Internal friction torque inside the rotary bearing $M_1 / KN \bullet m$	15

ISSN: 2414-1895 DOI: 10.6919/ICJE.202411_10(11).0005

By bringing the above parameters into (3), the erector torque M_2 under working condition 3 is $118KN•m$.

The fourth working condition: dynamic load 3 working condition. The first three motion conditions were all analyzed based on the vacuum suction cup grasping the segment, while the dynamic load condition 3 was no-load condition, that is, the vacuum suction cup did not grasp the segment. Under this working condition, the left and right sides of the erector lift the oil cylinder for rewinding action, while the rotary support for counterclockwise rotation movement, because of the no-load movement, the bottom does not have the gravity of the segment and seal side pressure, also subject to the internal friction torque of the rotary suppor. The working conditions of dynamic load 3 are shown in Figure 11 below. The mechanical diagram of dynamic load 3 is shown in the figure below. The mechanical diagram of dynamic load 3 is shown in the Figure 12 below.

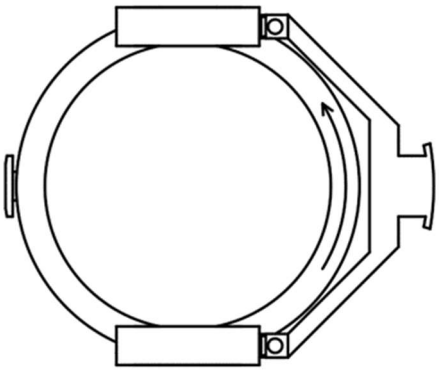

Figure 11. Working conditions 4

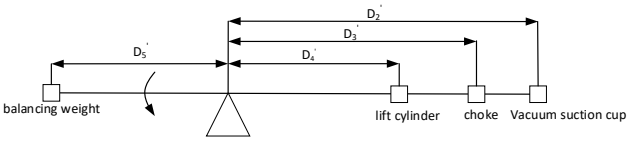

Figure 12. Schematic diagram of mechanical balance in working conditions 4

The final torque M_3 of the erector can be obtained from the mechanical diagram.

$$M_3 = (G_b \times D_2' + G_c \times D_3' + G_d \times D_4' - G_e \times D_5') / 100 + M_f \tag{4}$$

The meaning contained in mathematical expressions: G_b -The weight of the vacuum suction cup, KN ; D_2' -The distance from the center of gravity of the vacuum suction cup to the rotary center (hydraulic cylinder retraction stroke), mm ; G_c -The weight of the choke arm, KN ; D_3' -The distance from the support arm to the rotary center (hydraulic cylinder retraction stroke), mm ; G_d -The weight of the lifting hydraulic cylinder, KN ; D_4' -The distance from the lifting hydraulic cylinder to the rotary center (hydraulic cylinder retraction stroke), mm ; G_e -The weight of the top counterweight block, KN ; D_5' -The distance from the top counterweight block to the rotary center (hydraulic cylinder retraction stroke), mm ; M_f -Internal frictional torque of the slewing bearing, $KN•m$.

The design parameters are presented in Table 4 below:

ISSN: 2414-1895 DOI: 10.6919/ICJE.202411_10(11).0005

Table 4. Parameters under Operating Condition 4

Weight of the vacuum sucker G_b / T	0.9
The distance between the center of gravity of the vacuum chuck and the center of rotation $D_2^{'} / mm$	2125
Choke arm weight G_c / T	6
The distance from the choke arm to the center of rotation $D_3^{'} / mm$	1815
Lift the hydraulic cylinder weight G_d / T	6.8
Lift the hydraulic cylinder to the center of rotation $D_4^{'} / mm$	-213
Top counterweight weight G_e / T	4.7
The distance from the top weight weight to the center of rotation $D_5^{'} / mm$	2750
Internal friction torque inside the rotary bearing $M_1 / KN \bullet m$	15

Substituting the aforementioned parameters into equation (4), we find that the torque M_3 of the assembly machine under condition three is $14KN \bullet m$.

4. Static Analysis of the Frame Arm on the Assembly Machine

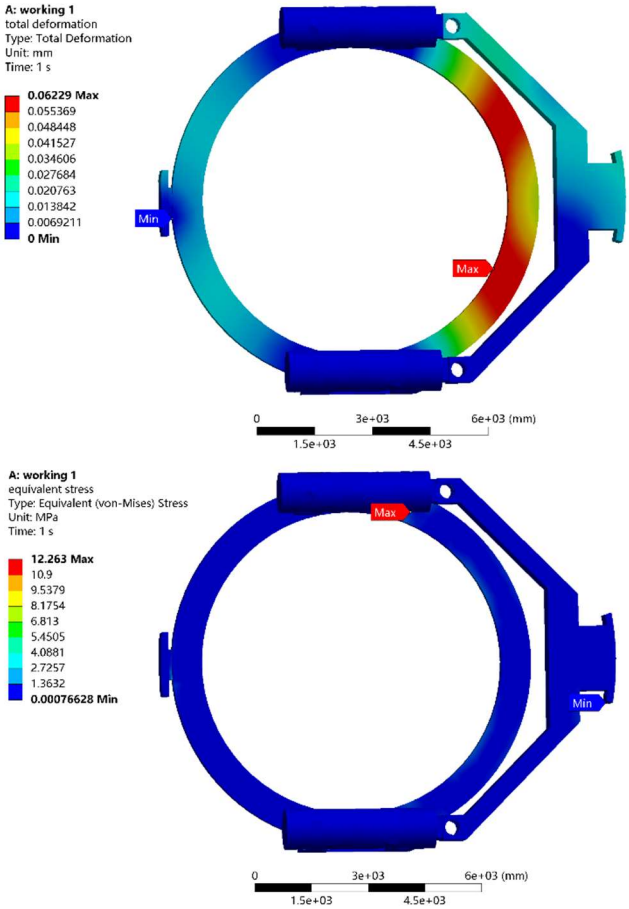

Figure 13. Displacement diagram and stress diagram of working condition 1

ISSN: 2414-1895 DOI: 10.6919/ICJE.202411_10(11).0005

The primary function of the gantry crane is to lift and move the pipe segments. It utilizes suction cups to adsorb and move the pipe segments to the specified location, ensuring precise placement to enhance the efficiency of the pipe segment installation and assembly. This study employs finite element analysis software to assess the load conditions on the choke frame across four specified working conditions. This assessment is based on the varying torques required for the assembly of pipe segments under different operational scenarios. Under four distinct operating conditions, the load exerted on the choke frame is distributed to the arm bodies and connection joints of its two end arms. Boundary conditions are imposed, and the choke frame is meshed, allowing us to determine its stress and deformation for each condition.

Condition 1: Stress and deformation cloud map of the assembly machine under no-load conditions.

Working condition 2: Structural stiffness analysis when the vacuum sucker grabs the tube segment and rotates to 90°. The diagram below shows the stress and deformation diagram under the load condition.

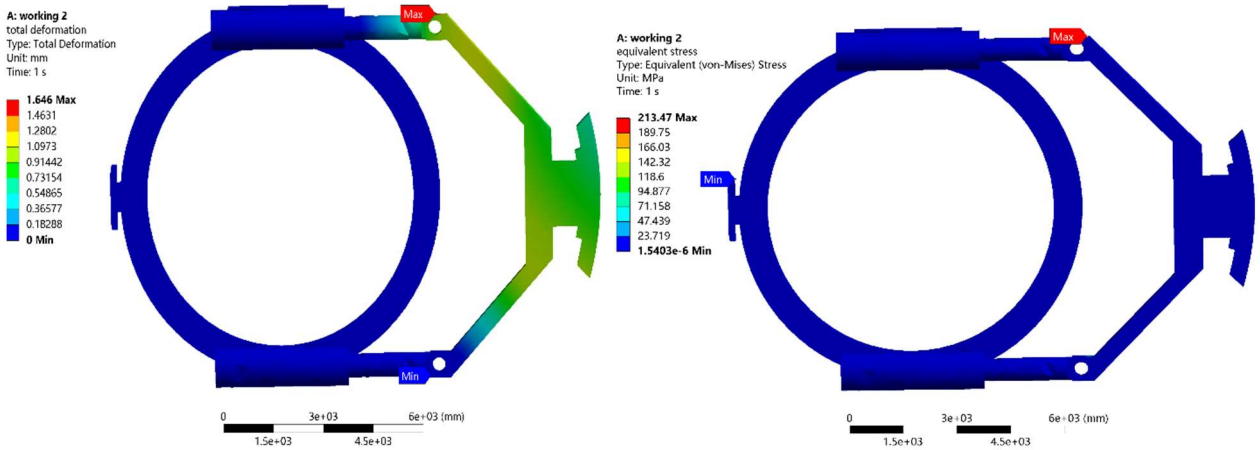

Figure 14. Displacement diagram and stress diagram of working condition 2

Working condition 3: The lifting hydraulic cylinder shrinks, and the vacuum sucker grabs the tube piece.

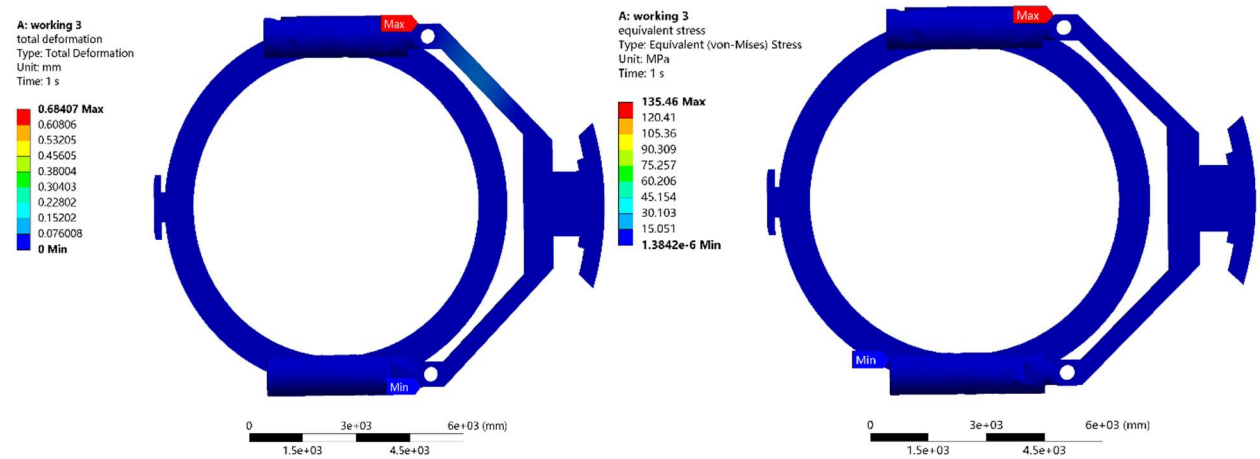

Figure 15. Displacement diagram and stress diagram of working condition 3

Working condition 3: Load condition analysis during the installation of the top pipe segment by the vacuum suction cup gripping the pipe segment for rotation.

ISSN: 2414-1895 DOI: 10.6919/ICJE.202411_10(11).0005

Figure 16. Displacement diagram and stress diagram of working condition 4

Through the stiffness analysis of the mechanism under the typical working conditions mentioned above, it can be concluded that under different poses and actions of grasping 4T pipe segments, the maximum displacement after loading is $1.65mm$ when the assembly machine rotates 90 ° under working condition two, located at the joint of the lifting arm, and the deformation is within a safe range. The maximum stress occurs at the connection between the choke and the hydraulic cylinder, which belongs to stress concentration, at 213.74 Mpa . The stress in most areas is less than 37 Mpa , which is lower than the yield strength of material Q355b (355 Mpa). Therefore, the stress is within the allowable stress range and the safety factor is relatively high. The stiffness of the choke is sufficient.

5. Conclusion

Currently, China's shield tunneling technology is rapidly advancing with machines trending toward larger diameters, demanding higher standards for the design of segment erectors. This paper, grounded in the requisite functions and actions of segment erectors, analyzes the stress conditions and grab structures under various loads and postures for calculation and study. Through the analysis and calculation of stress conditions in segment erectors, the rationality and accuracy of selections for functional components such as slewing bearings and drive systems are ensured. Additionally, mechanical property analyses and studies were conducted on the gantry frame under different working conditions, concluding that the stress and deformation remain within safe limits. The segment erector's overall strength and stiffness satisfy construction demands, ensuring a stable and reliable assembly process. This offers valuable insights for the manufacturing and processing of segment erectors.

Acknowledgments

This work was sponsored by Xinjiang national major engineering research project(EQ075/FY056).

References

[1] Jia Lianhui, Li Taiyun. Key technologies for ultra large diameter shield tunnel segment assembly machine [J]. Journal of Zhejiang University (Engineering Edition), 2020, 54 (04): 816-823.(In Chinese).

[2] Member Wu, Deng Bin, Wang Taoyong, et al. Automatic assembly method of shield tunnel segments based on line laser sensors [J]. Infrared and Laser Engineering, 2024, 53 (08): 75-87. (In Chinese).

[3] Hu Yanwei, Jia Lianhui, Li Ming. Development and application of horseshoe shaped shield tunnel segment assembly machine [J]. Tunnel Construction (Chinese and English), 2023, 43 (02): 327-333. (In Chinese).

ISSN: 2414-1895 DOI: 10.6919/ICJE.202411_10(11).0005

[4] Song Changbing. Optimization of translation mechanism design for pipe segment assembly machine [J]. Construction Machinery, 2022, (03): 76-78. DOI: 10.14189/j.cnki. cm 1981.2022.03.012. (In Chinese).

[5] Liu Feixiang. Research on the Intelligent Grasping and Assembly of Pipe Segment Assembling Machines [J]. Railway Construction, 2020, 60 (08): 58-63. (In Chinese).

[6] Xia Yimin, Hu Xinghuai, Mei Yongbing, et al. Mechanical properties of the choke frame for the assembly of a Φ 6.28m shield tunnel segment [J]. Mechanical Design and Research, 2012, 28 (06): 118-120+123. DOI: 10.13952/j.cnki. jofmdr. 2012.06.030. (In Chinese).

[7] Wang Daozhi, Min Rui, Yuan Xianghua, et al. Dynamic analysis of fine adjustment mechanism for shield tunnel segment assembly [J]. Journal of Tongji University (Natural Science Edition), 2024, 52 (06): 953-961. (In Chinese).

[8] Yuan Y C, Zhang Y. Building of fine-tuning mechanism posture and kinematics model for shield segment erector[J]. Advanced materials research, 2013, 634: 3737-3740.

[9] Duhme R, Rasanavaneethan R, Pakianathan L, et al. Theoretical basis of slurry shield excavation management systems[J]. Tunnelling and underground space technology, 2016, 57: 211-224.

[10] Duhme R, Rasanavaneethan R, Pakianathan L, et al. Theoretical basis of slurry shield excavation management systems[J]. Tunnelling and underground space technology, 2016, 57: 211-224.

[11] Li Suiting, Xie Xiaopeng, Zong Weiqi, et al. Vibration and Friction Analysis of Shield Tunnel Tube Assembling Machine [J]. Lubrication and Sealing, 2019,44 (02): 114-117+132. (In Chinese).